Comparison of classical methods for blade design and the influence of tip correction on rotor performance

Sørensen, Jens Nørkær; Okulov, Valery; Mikkelsen, Robert Flemming; Naumov, I. V.; Litvinov, I. V.

Published in:
Journal of Physics: Conference Series (Online)

Link to article, DOI:
10.1088/1742-6596/753/2/022020

Publication date:
2016

Document Version
Publisher's PDF, also known as Version of record

Comparison of classical methods for blade design and the influence of tip correction on rotor performance

2016 J. Phys.: Conf. Ser. 753 022020

(http://iopscience.iop.org/1742-6596/753/2/022020)

Comparison of classical methods for blade design and the influence of tip correction on rotor performance

J N Sørensen[1], **V L Okulov** [1,2], **R F Mikkelsen**[1], **I V Naumov**[2], **I V Litvinov**[2]

[1]Department of Wind Energy, Technical University of Denmark, 2800 Lyngby, Denmark
[2]Kutateladze Institute of Thermophysics, SB RAS, Novosibirsk 630090, Russia

E-mail: jnso@dtu.dk

Abstract. The classical blade-element/momentum (BE/M) method, which is used together with different types of corrections (e.g. the Prandtl or Glauert tip correction), is today the most basic tool in the design of wind turbine rotors. However, there are other classical techniques based on a combination of the blade-element approach and lifting-line (BE/LL) methods, which are less used by the wind turbine community. The BE/LL method involves different interpretations for rotors with finite or infinite numbers of blades and different assumptions with respect to the optimum circulation distribution. In the present study we compare the performance and the resulting design of the BE/M method by Glauert [1] and the BE/LL method by Betz [2] for finite as well as for infinite-bladed rotors, corrected for finiteness through the tip correction.
In the first part of the paper, expressions are given for the optimum design, including blade plan forms and local pitch distributions. The comparison shows that the resulting geometry of the rotor depends on the method used, but that the differences mainly exist in the inner part of the blade and at relatively small tip speed ratios (TSR<5). An important conclusion is that an infinite-bladed approach combined with a tip correction results in a geometry which is nearly identical to a geometry generated from a finite-bladed approach.
Next, the results from an experimental investigation on the influence on rotor performances of the tip correction on two different rotors are presented. Employing BE/M without the tip correction ("Glauert rotor") and BE/LL with the Goldstein's circulation ("Betz rotor") two different 3-bladed rotors were designed and manufactured. The two rotors were investigated experimentally in a water flume to compare their performance at different tip speed ratios and pitch angles. As a result of the comparison it was found that the Betz rotor had the best performance.

1. Introduction

Today almost all aerodynamic designs of wind turbine rotors rely on the blade-element/momentum theory as it was formulated in the 1930th by Glauert [1]. This model combines the blade-element approach with axisymmetric momentum theory, forming a model which essentially only is valid for infinite-bladed rotors. However, including a tip correction makes it possible to employ the theory to design practical finite-bladed rotors. On the other hand, there exists another class of methods, based on a combination of the blade-element approach and lifting-line (BE/LL) theory, which are less used by the wind turbine community. The BE/LL method involves different interpretations for rotors with finite or infinite numbers of blades and different assumptions with respect to the optimum circulation

distribution. In the model of Betz [2] a variational principle was employed to determine the optimum circulation distribution. Based on the criterion of Betz, a theory for finite-bladed rotors was developed by Goldstein [3] and later further developed by Okulov and Sørensen [4]. More details about the various models can be found in the surveys [5] and [6], and in the text book [7].

In the following we will derive the equations forming the basis for the two rotor models and employ them to make a comparative study on the rotor geometries and performance resulting from the two theories. In order to test and compare the resulting efficiency of the two design philosophies, the results from an experimental investigation on the influence on rotor performances on two different rotors will also be presented. Employing BE/M without the tip correction ("Glauert rotor") and BE/LL with the Goldstein's circulation ("Betz rotor") two different 3-bladed rotors were designed and manufactured. The two rotors were investigated experimentally in a water flume to compare their performance at different tip speed ratios and pitch angles.

2. Theory

In this section we outline the basic equations forming the aerodynamic design of optimum Glauert and Betz rotors, respectively.

2.1 Design of optimum Glauert rotor

The design model of Glauert is based on momentum theory applied on differential annular elements and various approximations. Of these, the most important is the assumption that the pressure change in the wake due to the swirl component of the velocity can be neglected. Without going in to details, the following expression is obtained from Glauert's analysis (see e.g. [1] or [7]):

$$a(1-a) = \lambda^2 x^2 a'(1+a'), \tag{1}$$

where the dimensionless interference coefficients are defined as

$$a = 1 - \frac{u_R}{U_0}, \quad a' = -\frac{u_\theta}{2r\Omega}, \tag{2}$$

with u_R denoting the axial velocity in the rotor plane, U_0 is the undisturbed wind speed, u_θ is the swirl velocity in a plane downstream of the rotor, Ω is the angular velocity of the rotor, and r is the axial position at the rotor plane. Furthermore, the tip speed ratio is defined as $\lambda = \frac{\Omega r}{U_0}$ and $x = \frac{r}{R}$, where R is the radius of the rotor. Interestingly, this equation can also be derived by assuming that the

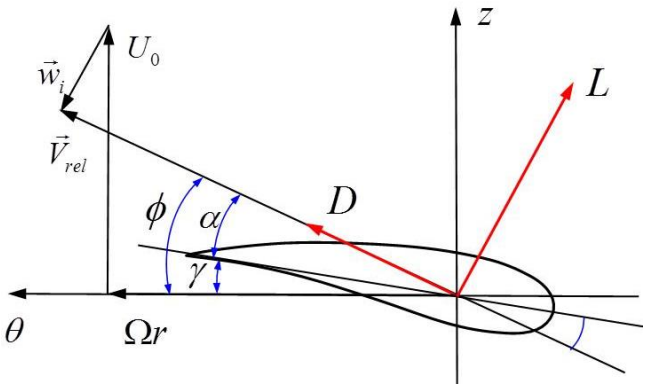

Figure 1. Cross-sectional element of airfoil showing the velocity triangle and flow angles.

relative velocity and the induced velocity are perpendicular in the rotor plane. This is shown in figure 1 which depicts a cross sectional element of a rotor blade with the velocity triangle inferred as vectors. Here the induced velocity is given as $\vec{w}_i = \left(-aU_0, a'r\Omega\right)$ and the relative velocity as $\vec{V}_{rel} = \left[(1-a)U_0, (1+a')r\Omega\right]$. Making the dot product between the two vectors and setting it equal to zero, results in eq. (1).

Introducing Euler's turbine equation on differential form, we get the following expression for the useful power produced by the wind turbine,

$$P = \Omega Q = \Omega \int_0^R 2\pi r^2 \rho u_R u_\theta dr = 4\pi\rho\Omega^2 R^4 U_o \int_0^1 a'(1-a)x^3 dx, \tag{3}$$

or in dimensionless form,

$$C_P \equiv \frac{P}{½\rho A U_0^3} = 8\lambda^2 \int_0^1 a'\left(1-a\right)x^3 dx, \tag{4}$$

By assuming that the different stream tube elements of the momentum analysis behave independently of each other, it is possible to optimize the integrand of eq. (4), $f(a,a') = a'(1-a)$, for each x separately. This result in the following relation for an optimum rotor (see [1] or [7]),

$$a' = \frac{1-3a}{4a-1}. \tag{5}$$

Combining eq. (1) with (5), the following equation is derived for the determining the optimum value of the axial interference factor,

$$16a^3 - 24a^2 + 3a(3-\lambda^2 x^2) - 1 + \lambda^2 x^2 = 0. \tag{6}$$

Solving eq. (6) for a given tip speed ratio, gives the distribution of the optimum axial interference factor, $a = a(x)$, along the blade. Having determined a, $a' = a'(x)$ is next computed from eq. (5), and the optimum power performance is finally computed by integration of eq. (4).

2.2 The tip correction

Since the equations forming the optimum Glauert rotor are based on axial momentum theory, they are only valid for rotors with infinitely many blades. In order to correct for finite number of blades, Glauert [1] introduced a tip loss factor, which essentially was derived by Prandtl in an appendix to the dissertation by Betz [2]. In this method a correction factor, $F = N_b\Gamma / \Gamma_\infty$, is introduced to correct the loading (circulation) between an infinite-bladed rotor and an N_b-bladed rotor. An approximate formula of the Prandtl tip loss function was introduced by Glauert [1] as follows,

$$F = \frac{2}{\pi}\cos^{-1}\left[\exp(-\frac{N_b(R-r)}{2r\sin\phi})\right], \tag{7}$$

where $\phi = \phi(r)$ is the angle between the local relative velocity and the rotor plane (see Fig. 1).

2.3 Design of optimum Betz rotor

For a rotor with a finite number of blades, Betz [2] showed that the ideal efficiency is obtained when the distribution of circulation along the blade produces a rigidly moving helicoidal vortex sheet with constant pitch, h, that moves in the direction of the undisturbed flow (in the case of a propeller) or against it (in the case of a wind turbine) with a constant velocity w (see Figure 2). Although Betz stated the problem of the wake, he was not able to solve the corresponding circulation distribution defining the rotor loading and rotor geometry. Part of the solution was later given by Goldstein [3] using infinite series of Bessel functions and recently a full solution was made by Okulov and Sørensen [4]. In the following, the different solution steps of the problem will be presented.

2.3.1 Kinematic properties

Denoting the angle between the vortex sheet and the rotor plane as Φ, the pitch is given as

$$h = 2\pi r \tan\Phi , \tag{8}$$

or, in dimensionless form,

$$l = h/2\pi R = (r/R)\tan\Phi , \tag{9}$$

where R is the radial extent of the vortex sheet. Since the vortex sheet is translated with constant relative axial speed, w, the induced velocity is identical to $w\cos\Phi$, which is the normal component to the screw surface (Figure 2).

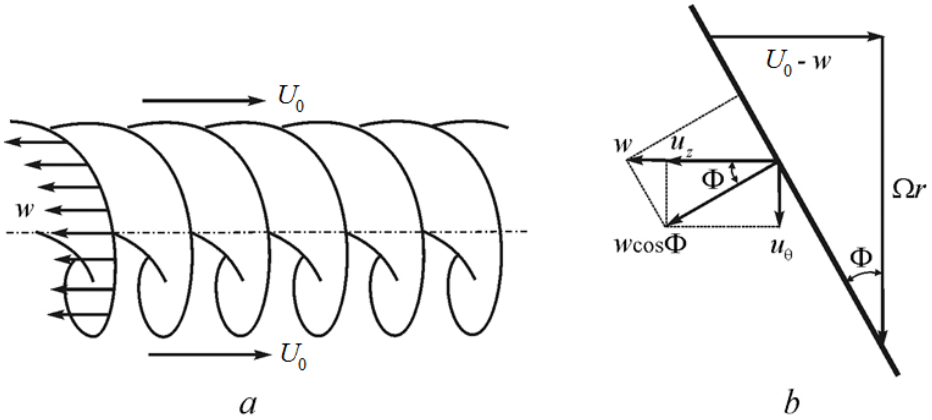

Figure 2. (a) Sketch of helical surface representing the ideal far wake; (b) Definition of axial displacement velocity of the helical vortex sheet and velocity triangles determining pitch angle and geometry of the helical surface. (Okulov and Sørensen [4]).

The axial and circumferential velocity components u_z and u_θ induced at the sheet itself are therefore given as (see Figure 2),

$$u_\theta = w\cos\Phi\sin\Phi \quad \text{and} \quad u_z = w\cos^2\Phi . \tag{10}$$

From simple geometric considerations these equations are rewritten as

$$u_\theta = wxl/\left(l^2 + x^2\right) \text{ and } u_z = wx^2/\left(l^2 + x^2\right), \tag{11}$$

where $x = r/R$ is the dimensionless radius, neglecting expansion of the wake.

Since the movement of the sheet is superposed on the undisturbed wind speed, U_0, it moves with axial velocity $U_0 - w$ and angular velocity Ω, and for any point on the n helical surfaces $(n = 1, 2, \ldots, N_b)$, we get

$$\theta = \Omega t + 2\pi(n-1)/N_b \quad \text{and} \quad z = (U_0 - w)t\,. \tag{12}$$

The angular pitch of the screw surface is thus given as

$$\tan\Phi = \frac{dz}{r d\theta} = \frac{U_0 - w}{\Omega r}, \tag{13}$$

and the dimensionless linear pitch is defined as

$$l \equiv x\tan\Phi = \frac{U_0}{\Omega R}(1 - \bar{w}), \tag{14}$$

where $\bar{w} = w/U_0$ is the dimensionless velocity of the sheet with respect to the surrounding fluid. Since each vortex sheet also defines a stream surface, the angular pitch can also be written

$$\tan\Phi = \frac{U_0 - u_z}{\Omega r + u_\theta}\,. \tag{15}$$

The above introduced parameters define the properties of an infinite sheet in the so-called Trefftz plane, which per definition is the plane normal to the relative wind infinitely far downstream of the rotor. It now remains to establish the characteristics in the rotor plane in order to utilize the Kutta–Joukowsky theorem to determine the loading. Assuming the wake to be in equilibrium and neglecting the rolling up of the sheet, as a consequence of Helmholtz' vortex theorem, the bound circulation Γ_0 about a blade element is uniquely related to the circulation Γ at a corresponding radius in the Trefftz plane. When the trailing wake from the initial deformation form regular helicoidal vortex surfaces, this relationship can be expressed as

$$\Gamma_0\left(\frac{r}{R_0}, l_0(\lambda_0)\right) = \Gamma\left(\frac{r}{R}, l\right), \tag{16}$$

where r/R_0 and r/R are the dimensionless radii in the rotor plane and at any cross section in the wake, respectively.

If the expansion of the wake is neglected, from symmetry, it is can be shown that the induced velocity in the rotor plane is half of the induced velocity in the far wake. A way of showing this, is to consider the induction in mid-plane of an infinitely long vortex sheet going from $-\infty$ to ∞. If half of the sheet is removed, such that the remaining part now forms a 'half-infinite' sheet going from 0 to ∞, then only the half induction takes place at the end plane (the former mid-plane). Thus, as a first order approximation we assume that

$$u_{\theta_0} = \tfrac{1}{2}u_\theta \quad \text{and} \quad u_{z_0} = \tfrac{1}{2}u_z\,. \tag{17}$$

In the rotor plane the angular pitch is given as

$$\tan\Phi_0 = \frac{U_0 - u_{z_0}}{\Omega_0 r + u_{\theta_0}} = \frac{U_0 - \frac{1}{2}u_z}{\Omega_0 r + \frac{1}{2}u_\theta} = \frac{\left(U_0 - \frac{1}{2}w\right)}{\Omega_0 r}\ , \tag{18}$$

where Ω_0 now denotes the angular speed of the rotor and $\Phi_0 (= \phi)$ is the flow angle in the rotor plane. The last equality in eq. (18) is not obvious, and we refer the reader to [8] for a formal proof. The linear pitch in the rotor plane written as

$$l_0 = \frac{r}{R_0}\tan\Phi_0 = \frac{U_0}{\Omega_0 R_0}\left(1 - \tfrac{1}{2}\overline{w}\right) = \frac{\left(1 - \frac{1}{2}\overline{w}\right)}{\lambda}. \tag{19}$$

2.3.2 Solution procedure

Goldstein [3] was the first who found an analytical solution to the potential flow problem of a moving infinite helical vortex sheet. In his model a dimensionless distribution of circulation was introduced as follows

$$G(x,l) = N_b \Gamma(x,l)/hw, \tag{20}$$

defining what later was designated the Goldstein circulation function. In the present work we solve the following matrix equation to determine the Goldstein function,

$$\left[\underline{\underline{A}}\right]\underline{\gamma} = \frac{x_i^2}{l^2 + x_i^2}, \tag{21}$$

where $\underline{\gamma} = \left[\gamma_1, \gamma_2, ..., \gamma_N\right]^T$ and $\gamma_i = \Gamma_i / w$, with $i \in \left[1, N\right]$. The elements in the matrix, a_{ij}, are defined by the induction from vortex element j on control point i, subject to a unit vortex strength, and are determined from the induction equations shown in [4].

Employing the Goldstein circulation function $G\left(x, l_0\right)$, now referring to quantities in the rotor plane, and introducing the linear pitch from Eq. (19), the total bound circulation in the rotor plane reads

$$N_b \Gamma_0\left(r, \lambda\left(l_0\right)\right) = w h_0\, G\left(r, l_0\right) = 2\pi R_0 l_0 w G(r, l_0) = 2\pi \frac{U_0^2}{\Omega_0}\overline{w}\left(1 - \tfrac{1}{2}\overline{w}\right) G\left(r, l_0\right). \tag{22}$$

Inserting eqs. (10), (17) and (22) into eq. (3), the power, $P = \Omega_0 Q$, can be determined from the following integral

$$P = 2\pi\rho V^3 \overline{w}(1 - \tfrac{1}{2}\overline{w}) R_0^2 \int_0^1 (1 - \tfrac{1}{2}\overline{w}\frac{x^2}{x^2 + l_0^2}) G x dx\,. \tag{23}$$

Performing the integration and introducing the dimensionless power coefficient (eq. 4), we get

$$C_P = 2\overline{w}\left(1 - \tfrac{1}{2}\overline{w}\right)\left(I_1 - \tfrac{1}{2}\overline{w} I_3\right), \tag{24}$$

where

$$I_1 = 2\int_0^1 G\left(x, l_0\right) x dx \quad \text{and} \quad I_3 = 2\int_0^1 G\left(x, l_0\right) \frac{x^3 dx}{x^2 + l_0^2}. \tag{25}$$

The coefficients I_1 and I_3 are usually referred to as the mass coefficient and the axial energy factor, respectively. For more details about the derivation and the behaviour of I_1 and I_3, we refer to [4]. For a given helicoidal wake structure, the power coefficients is seen to be uniquely determined, except for the parameter $\overline{w}$. Differentiation of C_P, eq. (24), with respect to $\overline{w}$ yields the maximum value of $C_{P,\max}$, resulting in

$$\overline{w}(C_P = C_{P,\max}) = \frac{2}{3I_3}\left(I_1 + I_3 - \sqrt{I_1^2 - I_1 I_3 + I_3^2}\right). \tag{26}$$

Combining eqs. (11) and (17), the following equation is obtained for determining the interference factors in the rotor plane,

$$a = ½\overline{w}\frac{x^2}{x^2 + l_0^2} \quad \text{and} \quad a' = ½\overline{w}\frac{l_0}{\lambda\left(x^2 + l_0^2\right)}. \tag{27}$$

2.4 Blade geometry

To determine the blade geometry of the designed rotor we employ the Kutta-Joukowsky theorem, from which we have the following expression,

$$N_b L = \rho V_{rel} \Gamma \Rightarrow N_b C_l = \frac{2\Gamma}{c V_{rel}}, \tag{28}$$

where N_b is the number of blades, L is the lift on each blade, C_l is the local lift coefficient, and Γ denotes the total circulation acting on the blades. From the circulation theorem we have $\Gamma = 2\pi r u_\theta$, which, combined with eq. (7), gives the following expression for the chord distribution,

$$c(r) = \frac{4\pi r u_\theta}{N_b C_l V_{rel}}. \tag{29}$$

Introducing the solidity, $\sigma \equiv \frac{N_b c}{2\pi R}$, and the interference factors defined in eq. (2), we get the following dimensionless expression for the planform of a rotor blade

$$\sigma C_l = \frac{4\lambda x^2 a'}{\sqrt{(1-a)^2 + \lambda^2 x^2 (1+a')^2}}. \tag{30}$$

This equation is quite general and will have to be associated with a set of equations for determining the distribution of the inference factors. From Figure 1 the local inflow angle is determined as,

$$\tan\phi = \frac{1-a}{\lambda x(1+a')}. \tag{31}$$

3. Comparison of blade geometries

In this section we compare the blade geometries for rotors designed using the equations derived in the previous section. Below we show some of the main results from the analysis.

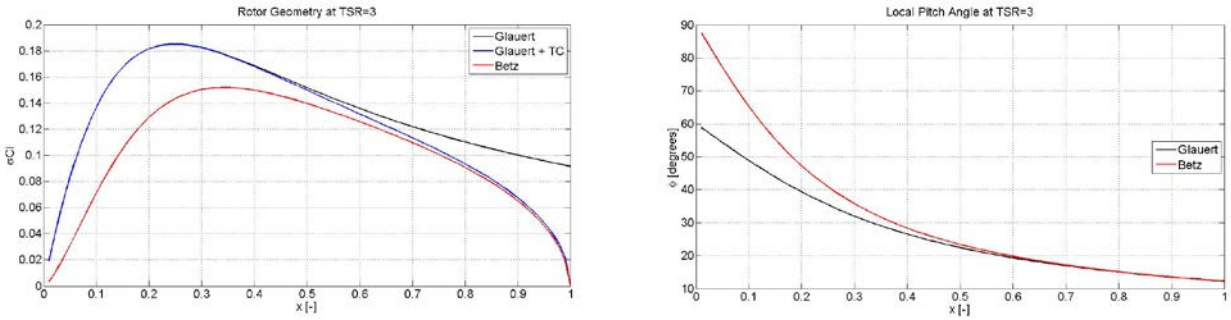

Figure 3. Comparison of chord and local pitch (twist) distributions for rotors at a tip speed ratio of 3.

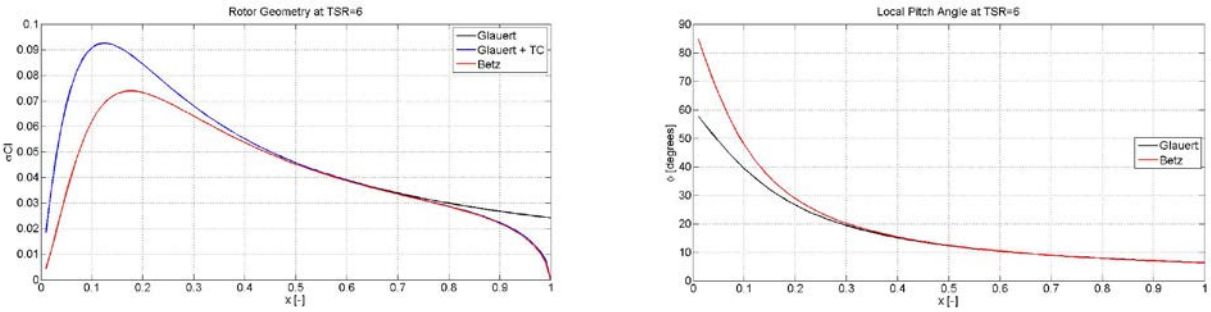

Figure 4. Comparison of chord and local pitch (twist) distributions for rotors at a tip speed ratio of 6.

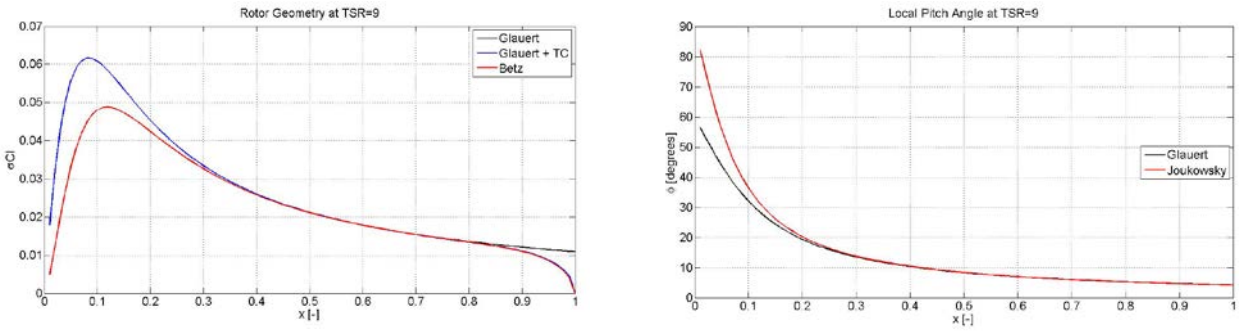

Figure 5. Comparison of chord and local pitch (twist) distributions for rotors at a tip speed ratio of 9.

In Figs. (3) – (5) blade plan forms and local pitch (twist) distributions are shown for rotors designed for tip speed ratios 3, 6 and 9, respectively. For the Glauert rotor, the blade plan form is shown both with and without tip correction. For a tip speed ratio of 3 (Fig. 3) large differences are seen more or less over the full span of the rotors. However, designing the rotor at a tip speed ratio 6 (Fig. 4), about 60 % of the outer part of the geometry is identical, independent of the employed aerodynamic model. Here it is also seen that the 'classical' Prandtl/Glauert tip correction indeed

represents a very good approximation to the full theoretical solution outlined by Betz. However, it is also seen that the inner parts are different. In particular this is the case for the local pitch angle, which in the Glauert model tends to 60^0, whereas it in the model of Betz becomes equal to 90^0 at the root section. In the Glauert case this can be deduced by evaluation of eqs. (1), (6) and (31), showing that $a = 1/4,\ 4\lambda x a' \to \sqrt{3}$, and $\tan\Phi \to \sqrt{3}$ for $x \to 0$. In the case of the Betz rotor, it follows directly from eq. (13) that $\Phi \to 90^0$ when the radius goes to zero. In general, the differences between the geometries disappear at high tip speed ratios, e.g. at a tip speed ratio of 9 (Fig. 5), the outer 75% of the blades are identical within plotting accuracy.

4. Experimental test of 3-bladed Glauert and Betz rotors

Two laboratory models of a 3-bladed rotor were designed with diameter D = 0.376m, a hub radius of 0.029m, and a blade of length 0.159m [9]. The blade chord and flow angle were determined at optimum operating conditions at a tip speed ratio λ = 5 using the BE/M without tip correction (Glauert's rotor) and BE/LL (Betz' rotor) theories, respectively. In Fig. 6 the measured power (C_P) and thrust (C_T) coefficients are compared as function of tip speed ratio for the two rotors. We will not here go into the details of the experiment, but just note that the Betz rotor achieved higher power and thrust coefficients at all operating tip speed ratios. The most likely reason for the difference is that the tip correction was not included in the design of the Glauert rotor. However, we do not have the full data to show if this is a general tendency or if it is only for the tip speed ratio for which the two turbines are designed (λ = 5). This will be the topic of a future study on aerodynamic design of optimum rotors.

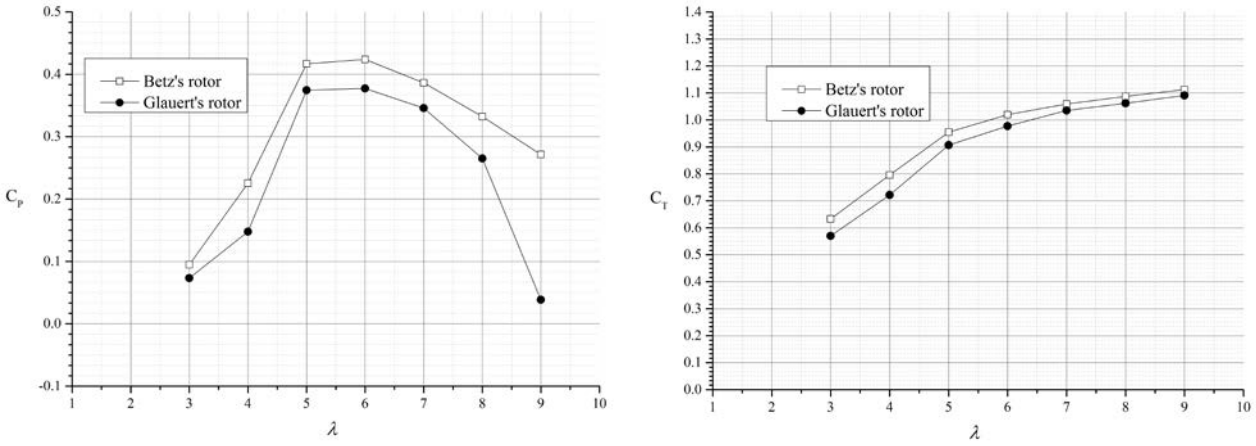

Figure 6. Experimental power and thrust coefficients of 3-bladed rotors designed using Glauert's model without tip correction and Betz's rotor with Goldstein's circulation distribution along the blades.

5. Conclusions

Two different design philosophies for designing optimum wind turbine rotors have been outlined and discussed. One of them (the Glauert rotor) is based on momentum theory whereas the other is based on lifting line or vortex theory (the Betz rotor). A comparison of the final design resulting from the rotor models shows that the main differences are to be found in the inner part of the rotor and that this difference is most pronounced at small and moderate tip speed ratios. Furthermore, a very positive

observation is that the approximate Prandtl/Glauert tip correction indeed represents the Goldstein circulation at the outer part of the rotor and that the classical infinite-bladed approximation with tip correction seems to be in very good agreement with the actual circulation distribution given by the Goldstein function.

A laboratory test of two different rotor designs, one based the infinite-bladed approach (Glauert rotor without tip correction) and one based on a finite-bladed approach (Betz rotor), demonstrated the importance of including the tip correction in the design.

Acknowledgments

The research was supported by the Danish Council for Strategic Research for the project Center for Computational Wind Turbine Aerodynamics and Atmospheric Turbulence (grant 2104-09-067216/DSF) (COMWIND: http://www.comwind.org) and the Russian Science Foundation (Project № 14-19-00487).

References

[1] Glauert, H. (1935) "Airplane propellers." *Aerodynamic Theory* (ed. Durand, W.F.), Dover Publication Inc., New York, Chapter VII, Div. L, pp. 251-268.
[2] Betz, A. (1919) "*Schraubenpropeller mit Geringstem Energieverlust."* Dissertation, Göttingen Nachrichten, Göttingen.
[3] Goldstein S. (1929) On the vortex theory of screw propellers. *Proc R Soc London* A; 123: 440–465.
[4] Okulov VL, Sørensen JN. (2008) Refined Betz limit for Rotors with a Finite Number of Blades. *Wind Energy*; 11(4): 415-426.
[5] Kuik GAM van, Sørensen JN, Okulov VL. (2014) The rotor theories by Professor Joukowsky: Momentum Theories. *Prog Aerospace Sci* 2015; 73: 1-18. DOI: 10.1016/j.paerosci.2014.10.
[6] Okulov VL, Sørensen JN, Wood DH. (2015) The rotor theories by Professor Joukowsky: Vortex Theories. *Prog Aerospace Sci*; 73: 19-46. DOI: 10.1016/j.paerosci.2014.10.002.
[7] Sørensen, J.N. (2016) "*General momentum theory for horizontal axis wind turbines*." Springer.
[8] Okulov, VL, Sørensen, JN. (2010) Maximum efficiency of wind tirbine rotors using Jokowsky and Betz approaches. *J. Fluid Mechanics*, vol. 649, pp. 497-508.
[9] Okulov VL, Naumov IV, Mikkelsen RF, Sørensen JN. (2015) Wake effect on a uniform flow behind wind-turbine model. *Journal of Physics Conference Series*; 625: 012011.